

Growth of low-frequency waves due to a photon beam in a magnetized electron–positron plasma

QINGHUAN LUO^{1,2†} and D. B. MELROSE²

¹Division of Space Geophysics, National Institute for Space Research, PO Box 515,
12201-970 S.J. Campos-SP, Brazil

²Research Centre for Theoretical Astrophysics, School of Physics, University of Sydney,
NSW 2006, Australia

(Received 25 June 1996 and in revised form 10 December 1996)

The effect of a beam of radio waves of very high brightness passing through a cold, magnetized, electron–positron plasma is discussed. The properties of the natural wave modes in such a plasma are summarized, and approximate forms for the nonlinear response tensor are written down. Photon-beam-induced instabilities of low-frequency waves in the pair plasma are analysed in the random-phase approximation. When three-wave interactions involve two high-frequency waves in the same mode and a low-frequency wave in a different mode, wave–wave interactions are similar to wave–particle interactions in that photons act like particles that emit and absorb low-frequency waves. The absorption coefficients for various low-frequency waves due to a photon beam are evaluated. In a pure electron–positron plasma, photon-beam-induced instabilities can be effective only when either the high-frequency or the low-frequency waves are strongly modified by the magnetic field. The growth of the low-frequency waves is most effective when the high-frequency photon beam has a frequency close to the cyclotron frequency.

1. Introduction

Induced three-wave interactions are important in astrophysical applications where radio emission of high brightness temperature is involved. Our particular interest is in pulsar winds (Luo and Melrose 1994) and eclipsing binary pulsar systems (Gedalin and Eichler 1993; Luo and Melrose 1995*a, b*), and there is related interest in an application to active galactic nuclei (Gangadhara and Krishan 1993; Levinson and Blandford 1994). At distances much larger than the size of the emission region, the intense radio beam is highly anisotropic, being confined to a small solid angle. The important effects associated with an anisotropic, high-brightness-temperature radio emission include the following: (i) the radio beam can cause the growth of low-frequency waves, e.g. Langmuir waves (Melrose 1994; Luo and Melrose 1994), *z*-mode waves (Luo and Melrose 1995*a*) or Bernstein waves (Luo and

† Present address: Department of Physics and Mathematical Physics, The University of Adelaide, SA 5005, Australia

Melrose 1995*b*), and (ii) the resulting low-frequency waves scatter the radio beam, resulting in eclipses (see e.g. Gedalin and Eichler 1993; Luo and Melrose 1995*a, b*), distortion of the spectrum (Levinson and Blandford 1994) or complete disruption of the beam. In the existing detailed treatments of the three-wave processes that lead to these effects, the ambient medium through which the photon beam propagates is assumed to be an electron–ion plasma. However, at least in the case where the photon beam propagates through a pulsar wind, the ambient medium is a highly relativistic, strongly magnetized electron–positron plasma. Our motivation for the investigation reported here is to explore the differences between photon-beam-induced instabilities in an electron–ion plasma and those in a magnetized electron–positron plasma. In this paper we restrict our attention to a simple case in which the ambient plasma is assumed to be a cold, magnetized electron–positron plasma. Although the cold-plasma assumption is unrealistic for a pulsar wind, this simpler case needs to be explored before considering a plasma with realistic particle distributions. The case of a cold, magnetized electron–positron plasma is some of interest in connection with laboratory experiments (see e.g. Surko *et al.* 1989; Greaves *et al.* 1994), and the properties of waves in such plasmas have received some attention in the recent literature (see e.g. Stewart and Laing 1992; Iwamoto 1993; Zank and Greaves 1995).

There is an extensive literature on the theory of wave–wave interactions in an electron–ion plasma (see e.g. Tsytovich 1977, and references therein), but the case of three-wave interactions in an electron–positron plasma has received relatively little attention, except for a few cases related to the application to pulsar radio emission (see e.g. Mikhailovskii 1980; Gedalin and Machabeli 1984; Istomin 1988). For an unmagnetized plasma, there is a major difference between an electron–ion plasma and an electron–positron plasma in the context of three-wave interactions: three-wave interactions are actually forbidden in a pure electron–positron plasma. The reason is that for a charge-neutral, unmagnetized electron–positron plasma, the electron and positron contributions to the quadratic nonlinear response are equal and opposite, and all physical processes, including three-wave interaction, that involve the quadratic nonlinearity are absent. In an actual electron–positron plasma three-wave coupling may occur owing either to a charge asymmetry, in the sense that the distributions of electrons and positrons are different in some way, or to the effect of the magnetic field. Here we investigate the latter effect, and consider three-wave interactions in a cold, *magnetized* electron–positron plasma, applying the results to low-frequency wave instabilities induced by an anisotropic photon beam traversing the plasma. Thus, in the three-wave processes that we consider, two of the waves (the unscattered and scattered radio photons) are of high frequency and are in the same wave mode, and the third wave is a low-frequency wave that may be driven unstable by the high-frequency waves. We treat the wave growth as negative absorption, assuming the random-phase approximation.

In Sec. 2 we write the linear and quadratic nonlinear response tensors for a cold, magnetized electron–positron plasma, and summarize relevant properties of the wave modes in such plasmas. In Sec. 3 we present a general formalism for photon-beam-induced instabilities and conditions for low-frequency wave growth. The absorption coefficients for various low-frequency waves are evaluated in Secs 4–6. The conclusions are summarized in Sec. 7.

2. The response of a cold, magnetized electron–positron plasma

In order to treat three-wave interactions in an electron–positron plasma, we need explicit expressions for (a) the properties of waves and (b) the nonlinear response tensor.

2.1. Weak-turbulence expansion

We define the response tensors by expanding the induced current in terms of the vector potential $A_i(\omega, \mathbf{k})$ of waves in the temporal gauge. This gives

$$J_i(\omega, \mathbf{k}) = \alpha_{ij}(\omega, \mathbf{k}) A_j(\omega, \mathbf{k}) + \int d\lambda \alpha_{ijs}(\omega, \mathbf{k}, \omega_1, \mathbf{k}_1, \omega_2, \mathbf{k}_2) A_j(\omega_1, \mathbf{k}_1) A_s(\omega_2, \mathbf{k}_2) + \dots, \quad (2.1)$$

where α_{ij} is the linear response tensor, α_{ijs} is the quadratic nonlinear response tensor and $d\lambda = d\omega_1 d^3k_1 d\omega_2 d^3k_2 \delta(\omega - \omega_1 - \omega_2) \delta^3(\mathbf{k} - \mathbf{k}_1 - \mathbf{k}_2)/(2\pi)^4$. It is often more convenient to describe the linear response in terms of the (dimensionless) effective dielectric permittivity tensor

$$K_{ij} = \delta_{ij} + \frac{1}{\omega^2 \varepsilon_0} \alpha_{ij}. \quad (2.2)$$

For a cold plasma, these tensors have the following forms (Melrose 1986):

$$K_{ij} = \delta_{ij} - \sum_{\pm} \frac{\omega_{p\pm}^2}{\omega^2} \tau_{ij}^{\pm}(\omega), \quad (2.3)$$

$$\alpha_{ijs} = - \sum_{\pm} \frac{\eta_{\pm} e^3 n_{\pm}}{2m_e^2} \left[\frac{k_r}{\omega_1} \tau_{rj}^{\pm}(\omega_1) \tau_{is}^{\pm}(\omega_2) + \frac{k_r}{\omega_2} \tau_{rs}^{\pm}(\omega_2) \tau_{ij}^{\pm}(\omega_1) + \frac{k_{1r}}{\omega} \tau_{ir}^{\pm}(\omega) \tau_{js}^{\pm}(\omega_2) + \frac{k_{2r}}{\omega} \tau_{ir}^{\pm}(\omega) \tau_{sj}^{\pm}(\omega_1) - \frac{k_{2r}}{\omega_1} \tau_{rj}^{\pm}(\omega_1) \tau_{is}^{\pm}(\omega) - \frac{k_{1r}}{\omega_2} \tau_{rs}^{\pm}(\omega_2) \tau_{ij}^{\pm}(\omega) \right], \quad (2.4)$$

where $\eta_+ = 1$ for positrons and $\eta_- = -1$ for electrons are the signs of the charges, and where n_{\pm} , $\omega_{p\pm} = (n_{\pm} e^2 / \varepsilon_0 m_e)^{1/2}$ are the corresponding number densities and plasma frequencies respectively. The other quantity introduced in (2.3) is

$$\tau_{ij}^{\pm}(\omega) = \frac{\omega^2}{\omega^2 - \Omega_e^2} \left(\delta_{ij} - \frac{\Omega_e^2}{\omega^2} \hat{B}_i \hat{B}_j + i\eta_{\pm} \frac{\Omega_e}{\omega} \varepsilon_{ijl} \hat{B}_l \right), \quad (2.5)$$

where $\hat{\mathbf{B}} = \mathbf{B}/B$ is a unit vector along the magnetic field \mathbf{B} , and $\Omega_e = eB/m_e$ is the electron (or positron) cyclotron frequency. In (2.5), ε_{ijl} is the permutation symbol ($= 1$ for an even permutation of ijl , -1 for an odd permutation, and 0 otherwise).

2.2. The linear response

In a coordinate system in which \mathbf{B} is along the z axis and the wave vector \mathbf{k} is in the (x, y) plane, the linear response tensor has a form similar to that for a cold electron plasma (see e.g. Stix 1962; Melrose 1986). We write (2.3) with (2.5) in the form

$$K_{xx} = K_{yy} = 1 - \frac{X}{1 - Y^2}, \quad (2.6a)$$

$$K_{xy} = -K_{yx} = i\xi \frac{XY}{1 - Y^2}, \quad (2.6b)$$

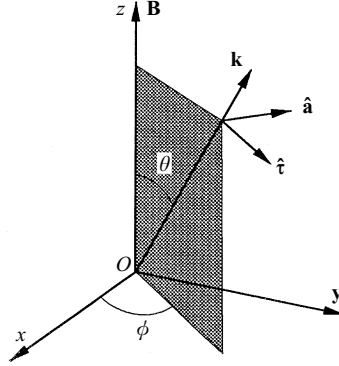


Figure 1. Definition of unit vectors $\hat{\mathbf{t}}$, $\hat{\mathbf{a}}$ and $\hat{\mathbf{k}}$ in terms of the Cartesian coordinates (x, y, z) . For low-frequency waves, the three vectors are relabelled as $\hat{\mathbf{t}}_2$, $\hat{\mathbf{a}}_2$, $\hat{\mathbf{k}}_2$. The magnetic field \mathbf{B} is in the z direction.

$$K_{zz} = 1 - X, \quad K_{xz} = K_{zx} = K_{yz} = K_{zy} = 0, \quad (2.6c)$$

with $X = \omega_p^2/\omega^2$, $\omega_p^2 = \omega_{p+}^2 + \omega_{p-}^2$ and $Y = \Omega_e/\omega$, and where $\xi = (n_+ - n_-)/(n_+ + n_-)$ is a measure of the charge imbalance. In the following discussion we assume $\xi = 0$, in which case the response tensor K_{ij} is diagonal. This implies that a cold, magnetized electron–positron plasma is non-gyrotropic (Stewart and Laing 1992).

2.3. Specific wave modes

We summarize the wave modes in a cold, magnetized electron–positron plasma and then comment on the relation between our results and those of earlier authors (Stewart and Laing 1992; Iwamoto 1993; Zank and Greaves 1995).

Wave properties. We describe the waves in terms of three wave properties: the dispersion relation, the polarization vector and the ratio of electric to total energy. The dispersion relation for a wave mode σ is expressed in terms of the refractive index $n_\sigma(\omega, \theta)$ as a function of frequency and angle of propagation, except for longitudinal waves, which in a cold plasma formally correspond to resonances, that is, infinities in the refractive index. For a gyrotropic medium, such as a magnetized electron gas, the wave polarization can be written in the form (see e.g. Melrose 1986, p. 168)

$$\mathbf{e}_\sigma = \frac{L_\sigma \hat{\mathbf{k}} + T_\sigma \hat{\mathbf{t}} + i\hat{\mathbf{a}}}{(1 + T_\sigma^2 + L_\sigma^2)^{1/2}}, \quad (2.7)$$

where T_σ and L_σ are the transverse and longitudinal polarization coefficients respectively, and σ labels the wave mode. The three base vectors as shown in Fig. 1 are given by $\hat{\mathbf{k}} = \mathbf{k}/k = (\sin \theta \cos \phi, \sin \theta \sin \phi, \cos \theta)$, $\hat{\mathbf{t}} = (\cos \theta \cos \phi, \cos \theta \sin \phi, -\sin \theta)$ and $\hat{\mathbf{a}} = (-\sin \phi, \cos \phi, 0)$. The distinguishing feature of a gyrotropic medium is that one of the components of the electric vector, here the component along $\hat{\mathbf{a}}$, is out of phase with the other two. An electron–positron gas with $\xi = 0$ is not gyrotropic, and the polarization vectors (apart from an arbitrary phase) are real. They correspond to the special cases $L_\sigma = 0 = T_\sigma$, giving $\mathbf{e}_\sigma = \hat{\mathbf{a}}$, and $L_\sigma = \infty = T_\sigma$, implying that \mathbf{e}_σ is in the $(\hat{\mathbf{k}}, \hat{\mathbf{t}})$ plane (the (x, z) plane for $\phi = 0$).

The ratio of the electric energy to the total energy in the σ -mode waves is (Melrose

1986, p. 169)

$$R_\sigma = \frac{\omega}{\partial[\omega^2 K_\sigma(\omega, \mathbf{k})]/\partial\omega}\bigg|_\sigma, \quad (2.8)$$

with $K_\sigma = e_{\sigma i}(\mathbf{k}) K_{ij}(\omega, \mathbf{k}) e_{\sigma j}^*(\mathbf{k})$, and where the subscript σ corresponds to the dispersion relation of mode σ being used.

The analogy with a uniaxial crystal. The response tensor (2.6a-c) for $\xi = 0$ is of the same form as for a uniaxial crystal, with $K_\perp = K_{xx} = K_{yy}$ and $K_\parallel = K_{zz}$. The dispersion relations for the ordinary and extraordinary modes for a uniaxial crystal are well known (see e.g. Melrose and McPhedran 1991, p. 147). However, the labelling of the modes is opposite to that conventionally adopted in the magnetoionic theory. In writing down the following solutions, we adopt the magnetoionic convention (the ordinary mode is defined to be the mode that has dispersion relation $n_o^2 = 1 - X$ for $\theta = \frac{1}{2}\pi$.)

Extraordinary-mode waves. The extraordinary (x) mode has dispersion relation $n_x^2 = K_\perp$, which gives

$$n_x^2 = 1 - \frac{X}{1 - Y^2}. \quad (2.9)$$

These waves can propagate for $\omega > \omega_H$ (where $\omega_H^2 = \omega_p^2 + \Omega_e^2$ is the upper-hybrid frequency) or $\omega < \Omega_e$, and are evanescent in a stop band between a resonance at Ω_e and a cutoff at ω_H . Their polarization vector $\mathbf{e}_x = \hat{\mathbf{a}}$ is strictly transverse. From (2.8), the ratio of electric to total energy in the x mode is derived as

$$R_x = \frac{1}{2} \left[1 + \frac{XY^2}{(1 - Y^2)^2} \right]^{-1}. \quad (2.10)$$

For $X \ll 1$ and $Y \ll 1$, we have $R_x \approx \frac{1}{2}$.

Ordinary-mode waves. The ordinary (o) mode has dispersion relation

$$n_o^2 = \frac{(1 - X - Y^2)(1 - X)}{1 - X - Y^2 + XY^2 \cos^2 \theta}. \quad (2.11)$$

The polarization vector of the o mode is

$$\begin{aligned} \mathbf{e}_o &= \frac{(K_\parallel \cos \theta, 0, -K_\perp \sin \theta)}{(K_\parallel^2 \cos^2 \theta + K_\perp^2 \sin^2 \theta)^{1/2}} \\ &= \frac{((1 - X - Y^2 + XY^2) \cos \theta, 0, -(1 - X - Y^2) \sin \theta)}{[(1 - X - Y^2 + XY^2)^2 \cos^2 \theta + (1 - X - Y^2)^2 \sin^2 \theta]^{1/2}}. \end{aligned} \quad (2.12)$$

The ratio of electric to total energy in the o mode can be derived from (2.8) in the same way as for (2.10). The expression for R_o is lengthy and we only write down its approximation (up to $X/Y^2 \ll 1$) for $Y \gg 1$ as

$$R_o \approx \frac{1}{2} \left[1 - \frac{(1 - X)^2 \cos^2 \theta}{(1 - X)^2 \cos^2 \theta + \sin^2 \theta} XY^{-2} \right]. \quad (2.13)$$

The corresponding dispersion relation is approximated by $n_o^2 \approx (1 - X)/(1 - X \cos \theta)$.

Longitudinal waves. The longitudinal part of the linear response tensor is unaffected by the gyrotropy (the $K_{xy} = -K_{yx}$ term for a cold electron gas). Hence the properties of Langmuir waves in a cold, magnetized pair plasma are identical to those in a cold, magnetized electron gas. For propagation along the magnetic field, Langmuir waves have frequency $\omega = \omega_p$ (plus the usual thermal correction $3k^2 V_e^2/2\omega_p$ in practice). At arbitrary angle θ there are two solutions with frequencies given by (see e.g. Melrose 1986, p. 171)

$$\omega_{\pm}^2(\theta) = \frac{1}{2}(\omega_p^2 + \Omega_e^2) \pm \frac{1}{2}[(\omega_p^2 + \Omega_e^2)^2 - 4\omega_p^2\Omega_e^2 \cos^2 \theta]^{1/2}, \quad (2.14)$$

with the upper frequency solution corresponding to Langmuir waves for $\Omega_e < \omega_p$. For perpendicular propagation ($\theta = \frac{1}{2}\pi$) one has $\omega_+(\frac{1}{2}\pi) = \omega_H$ and $\omega_-(\frac{1}{2}\pi) = 0$. For parallel propagation, $\omega_{\pm}(0)$ reduce to the maximum and minimum of ω_p and Ω_e respectively. The two frequencies (2.14) correspond to resonances in the cold plasma modes, and both resonances occur in the o mode.

For longitudinal waves $\sigma = l$, we have $\mathbf{e}_l = \hat{\mathbf{k}} \equiv \mathbf{k}/k$ and $K_l(\omega, \mathbf{k}) = (1 - X - Y^2 + XY^2 \cos^2 \theta)/(1 - Y^2)$. Using (2.8), we obtain

$$R_l = \frac{1}{2} \left[1 + \frac{XY^2}{(1 - Y^2)^2} \sin^2 \theta \right]^{-1}. \quad (2.15)$$

For the special cases of parallel propagation ($\theta \rightarrow 0$), the weak-field limit $Y \rightarrow 0$ and the strong-field limit $Y \rightarrow \infty$, we have $R_l \rightarrow \frac{1}{2}$.

Comparison with earlier results. Our results agree with the cold-plasma results of Stewart and Laing (1992), who concentrated on the case $\Omega_e \ll \omega_p$. There are some differences between our results and those of Zank and Greaves (1995), who included thermal effects through pressure terms, relating to how different branches of the modes link across resonances. Such differences are known to occur between the cold-plasma and thermal-fluid treatments of waves in electron-ion plasmas (see e.g. Stringer 1963), and we comment on them no further here. The results of Iwamoto (1993), who considered only parallel and perpendicular propagation in a cold plasma, differ in subtle ways from our results. In fact, both the parallel and perpendicular cases are singular in a cold pair plasma. The case of parallel propagation is special, because the polarization of the modes depends on how the limit of parallel propagation is taken. Iwamoto (1993) argued that if one solves for the wave properties assuming parallel propagation then the polarization is either circular or longitudinal. Technically, this is correct if one takes the limit as $\theta \rightarrow 0$ before taking $\xi \rightarrow 0$. These two limits do not commute, and we are considering a plasma with $\xi = 0$ here. Similarly, the case of perpendicular propagation is singular. For $\theta \neq \frac{1}{2}\pi$, the resonances at the frequencies (2.14), which correspond to $1 - X - Y^2 + XY^2 \cos^2 \theta = 0$, are obviously in the o mode, cf. (2.11). However, for $\theta = \frac{1}{2}\pi$ the denominator cancels with the first factor in the numerator in (2.11), and there is no resonance in the o mode. On the other hand, there is a resonance in the lower branch of the x mode (2.9) at $\omega = \Omega_e$ for all angles of propagation. Iwamoto (1993), who noted that one of the resonant frequencies (2.14) reduces to Ω_e for $\theta = \frac{1}{2}\pi$, argued that this resonance in the x mode be identified with the lower-hybrid resonance. The cyclotron resonance in the x mode at $\omega = \Omega_e$ is not longitudinal, and so should not be identified as the counterpart of the lower-hybrid resonance.

Finally, we comment on the cyclotron resonance in the case $\Omega_e \gg \omega_p$. As in an

electron plasma, there is a resonance in the o mode at $\omega_+(\theta)$, which approaches Ω_e as θ approaches zero. In a pair plasma there is also a resonance in the x mode, exactly at Ω_e . Above each of these resonances, in the cold-plasma limit, there is a narrow stop band in the relevant mode. Thermal effects can wash out such paired resonances and stop bands. The resonance and stop band are entirely washed out for $V_e/c \gtrsim \omega_p^2/\Omega_e^2$ (see e.g. Stix 1962), where V_e is the thermal speed of electrons and where we assume $\Omega_e \gg \omega_p$. In discussing the high-frequency waves below, we assume that this condition is satisfied.

2.4. The quadratic nonlinear response

In the expression (2.4) for the quadratic nonlinear response tensor, for a charge-neutral electron–positron plasma ($\xi = 0$), the sum over the two signs of the charge leads to cancellation of a large number of terms. The resulting expression for $\xi = 0$ is given by (A 1) in Appendix A. The general form (A 1) is too cumbersome for most purposes, and approximations need to be made.

We assume that the frequency ω_2 of the low-frequency waves is much smaller than the frequencies $\omega \approx \omega_1$ of the high-frequency waves, we set $\omega_1 = \omega - \omega_2$, and we retain only the leading term in an expansion in ω_2 . In addition, we consider only limiting cases of the magnetic field: either the magnetic field is weak, $\Omega_e, \omega_2 \ll \omega$, or it is strong $\Omega_e, \omega \gg \omega_2$. We also assume that the high-frequency waves are transverse and their polarization vectors are real (apart from an arbitrary phase).

For the weak-field case, the quadratic response tensor can be expanded in the form (see Appendix A)

$$\alpha_{ijs} \approx -i \frac{\varepsilon_0 e \omega_p^2}{2m_e c} \frac{n_2 \omega_2 \Omega_e}{\omega_2^2 - \Omega_e^2} \delta_{ij} \hat{a}_{2s} \sin \theta_2, \quad (2.16)$$

with $n_2 = k_2 c / \omega_2$ and $\hat{\mathbf{a}}_2 = (-\sin \phi_2, \cos \phi_2, 0)$ (see Fig. 1), and where (θ_2, ϕ_2) are the polar angles of \mathbf{k}_2 relative to \mathbf{B} . In deriving (2.16), we omit all terms that would contribute to order ω_2^2/ω^2 and higher in $e_i^* e_{1j} \alpha_{ijs} e_{2s}$.

For the strong-field case, the quadratic response tensor can be written as

$$\alpha_{ijs} = -i \frac{\varepsilon_0 e \omega_p^2}{2m_e c} \frac{n \omega \Omega_e}{\omega^2 - \Omega_e^2} \left[(\hat{a}_j \hat{B}_i - \hat{a}_i \hat{B}_j) \hat{B}_s \sin \theta \right. \\ \left. + \left(\frac{\omega^2 + \Omega_e^2}{\omega^2 - \Omega_e^2} \cos \theta + \frac{n_2}{n} \cos \theta_2 \right) \varepsilon_{ijl} \hat{B}_l \hat{B}_s + \frac{\omega_2}{\omega} P_{ijs} \right], \quad (2.17)$$

where (θ, ϕ) are the polar angles of \mathbf{k} with respect to \mathbf{B} . The first and second terms in (2.17) are antisymmetric under the interchange of i and j , and hence contribute only to order ω_2/ω in $e_i^* e_{1j} \alpha_{ijs} e_{2s}$ under the assumptions made here. The full expression for the factor P_{ijs} in the final term in (2.17) is given by (A 6). Here we write down its approximation only for $\omega \ll \Omega_e$, which is

$$P_{ijs} = \frac{n_2}{n} \hat{a}_{2i} \hat{B}_j \hat{B}_s \sin \theta_2, \quad (2.18)$$

where $\hat{\mathbf{a}}$ is defined as in (2.7).

Finally, consider the case in which the high-frequency photon beam is near the cyclotron resonance. For $|\omega^2 - \Omega_e^2| \ll 2\omega\omega_2$, the terms involving $1/(\omega^2 - \Omega_e^2)$ dominate.

From (A 7) and (A 8) we have

$$\alpha_{ijs} = -i \frac{\varepsilon_0 e \omega_p^2}{2m_e c} \frac{n\omega\Omega_e}{\omega^2 - \Omega_e^2} \frac{\omega}{\omega_2} \left\{ -\varepsilon_{ijl} \hat{B}_l \hat{B}_s \cos \theta \right. \\ \left. + \frac{\omega_2}{\omega} \left[(d_{ij} \hat{a}_s - \hat{a}_i \hat{B}_j \hat{B}_s) \sin \theta - \frac{n_2}{n} \hat{k}_{2r} (d_{ir} \varepsilon_{sjl} + d_{sj} \varepsilon_{irl}) \hat{B}_l \right] \right\}, \quad (2.19)$$

with $d_{ij} = \delta_{ij} - (\omega^2/\Omega_e^2) \hat{B}_i \hat{B}_j$.

3. Photon-beam-induced instabilities

In the following discussion the high-frequency waves are described by their frequency ω , wave vector \mathbf{k} and occupation number $N(\mathbf{k})$, and the low-frequency waves are described by ω_2 , \mathbf{k}_2 and $N_L(\mathbf{k}_2)$.

3.1. Quasilinear equations

We consider the small-angle scattering approximation, $k \approx k_1 \gg k_2$, in which the two high-frequency waves are in the same mode and are interpreted as the unscattered and scattered waves. In the small-angle scattering approximation, kinetic equations for the three waves reduce to equations that resemble the quasilinear equations for wave-particle interactions, given by (for details see Appendix B)

$$\frac{dN}{dt} = \frac{\partial}{\partial k_i} \left(D_{ij} \frac{\partial N}{\partial k_j} + G_i N^2 \right), \quad (3.1)$$

$$\frac{dN_L}{dt} = -\Gamma N_L + S, \quad (3.2)$$

with

$$\Gamma = - \int \frac{d^3 k}{(2\pi)^3} w(\mathbf{k}, \mathbf{k}_2) k_{2i} \frac{\partial N}{\partial k_{2i}}, \quad (3.3)$$

$$S = \int \frac{d^3 k}{(2\pi)^3} w(\mathbf{k}, \mathbf{k}_2) N^2, \quad (3.4)$$

$$D_{ij} = \int \frac{d^3 k_2}{(2\pi)^3} w(\mathbf{k}, \mathbf{k}_2) k_{2i} k_{2j} N_L(\mathbf{k}_2), \quad (3.5)$$

$$G_i = \int \frac{d^3 k_2}{(2\pi)^3} w(\mathbf{k}, \mathbf{k}_2) k_{2i}, \quad (3.6)$$

where $w(\mathbf{k}, \mathbf{k}_2)$ is the probability of emission of a low-frequency wave by a high-frequency photon, which can be expressed in terms of the quadratic response tensor α_{ijl} as

$$w(\mathbf{k}, \mathbf{k}_2) = \frac{4\hbar R R_1 R_2 |e_i^* e_{1j} e_{2l} \alpha_{ijl}|^2}{\varepsilon_0^3 \omega \omega_1 \omega_2} \Bigg|_{\mathbf{k}_1 = \mathbf{k} - \mathbf{k}_2} 2\pi \delta(\omega_2 - \mathbf{k}_2 \cdot \mathbf{v}_g), \quad (3.7)$$

with $\omega = \omega(\mathbf{k})$, $\omega_1 \approx \omega(\mathbf{k}_1)$, $|\mathbf{k}_1| \approx |\mathbf{k}|$, $R_1 \approx R$ and $\mathbf{v}_g = \partial\omega(\mathbf{k})/\partial\mathbf{k}$ for the high-frequency waves.

The terms involving Γ in (3.2) and D_{ij} in (3.1) describe the effects of stimulated emission and absorption of the low-frequency waves by the high-frequency waves, and are direct counterparts of the analogous terms that describe stimulated emission and absorption of waves by particles in the usual quasilinear equations. The

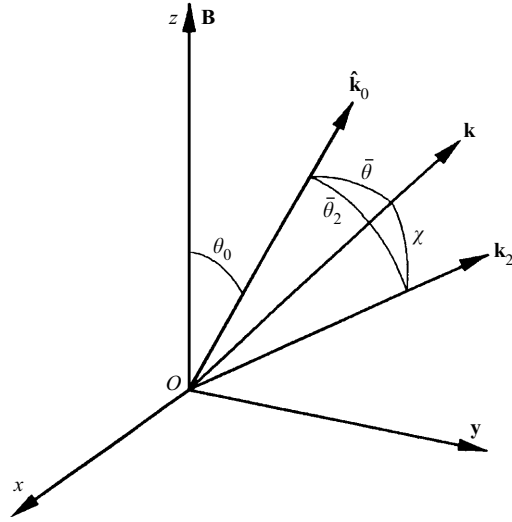


Figure 2. Photon-beam axis $\hat{\mathbf{k}}_0$, and high- and low-frequency wave vectors \mathbf{k} and \mathbf{k}_2 . As in Fig. 1, the magnetic field \mathbf{B} is in the z direction.

term S in (3.2) and the term proportional to G_i in (3.1) describe the effects of emission of a low-frequency wave due to induced photon decay, which may be regarded as the counterpart of spontaneous emission in a wave-particle interaction (cf. (6.42) and (6.43) in Melrose 1986). Both terms are proportional to N^2 , and this reflects the nonlinear nature of the three-wave process, which is qualitatively different from the wave-particle counterpart.

3.2. Conditions for growth

First consider the condition for exponential growth. Equation (3.2) can be formally integrated to yield

$$N_L = \int^t dt' S \exp\left(\int^{t'} \Gamma dt''\right) \exp\left(-\int^t \Gamma dt''\right). \tag{3.8}$$

Let $|\Gamma|_{\max}$ and ΔL be the maximum growth rate and the scattering length scale respectively. Then the condition for exponential growth is

$$|\Gamma|_{\max} \Delta L / c \gtrsim 1. \tag{3.9}$$

Assuming that within $\Delta L = \Delta t c$ along the line of sight the plasma parameters are uniform and Γ is negative, one has

$$N_L = -\frac{S}{\Gamma} \exp(-\Gamma \Delta t). \tag{3.10}$$

For $|\Gamma|_{\max} \Delta L / c \ll 1$, induced photon decay needs to be taken into account, and then, in place of (3.10), one has $N_L = S \Delta t$.

Next consider the detailed condition for growth of the low-frequency waves, that is, for negative absorption, $\Gamma < 0$. To evaluate the absorption coefficient (3.3), we assume that the photon beam is axisymmetric. Let $(\bar{\theta}, \bar{\phi})$ and $(\bar{\theta}_2, \bar{\phi}_2)$ be the polar angles of \mathbf{k} and \mathbf{k}_2 respectively with respect to the axis of the photon beam, as shown in Fig. 2. The corresponding unbarred angles are with respect to the direction of

the magnetic field. Then the absorption coefficient (3.3) becomes

$$\Gamma = - \int d\bar{\phi} \int d\bar{\theta} \sin \bar{\theta} \int \frac{k^2 dk}{(2\pi)^2} \bar{u} \delta[k_2 v_g (\cos \chi - \cos \chi_0)] \times \left(k_2 \cos \chi \frac{\partial}{\partial k} + k_2 \frac{\cos \bar{\theta} \cos \chi - \cos \bar{\theta}_2}{k \sin \bar{\theta}} \frac{\partial}{\partial \bar{\theta}} \right) N(k, \bar{\theta}), \quad (3.11)$$

with $\cos \chi = \cos \bar{\theta} \cos \bar{\theta}_2 + \sin \bar{\theta} \sin \bar{\theta}_2 \cos(\bar{\phi} - \bar{\phi}_2)$, and where

$$\bar{u} = \frac{4\hbar R R_1 R_2 |e_i^* e_{1j} e_{2l} \alpha_{ijl}|^2}{\varepsilon_0^3 \omega \omega_1 \omega_2} \Bigg|_{\mathbf{k}_1 = \mathbf{k} - \mathbf{k}_2}. \quad (3.12)$$

The angle $\chi_0 = \arccos(\omega_2/k_2 v_g)$ is the Čerenkov angle, which defines an interface between the regions $v_{2\phi} \equiv \omega_2/k_2 < v_g \approx c$ and $v_{2\phi} > v_g \approx c$. Let Γ_k and Γ_a be the terms involving k and angular derivatives respectively. Thus, for a highly collimated photon beam, the absorption coefficient (3.11) can be written into the form $\Gamma = \Gamma_k + \Gamma_a$, with (Appendix C)

$$\Gamma_k = - \int \frac{\bar{\theta} d\bar{\theta} k^2 dk}{(2\pi)^2} \frac{\bar{u}}{c} \frac{\cot \chi_0}{[\bar{\theta}^2 - (\bar{\theta}_2 - \chi_0)^2]^{1/2}} \frac{\partial N}{\partial k}, \quad (3.13a)$$

$$\Gamma_a = - \int \frac{d\bar{\theta} k dk}{(2\pi)^2} \frac{\bar{u}}{c} \frac{\bar{\theta}_2 - \chi_0}{[\bar{\theta}^2 - (\bar{\theta}_2 - \chi_0)^2]^{1/2}} \frac{\partial N}{\partial \bar{\theta}}. \quad (3.13b)$$

We consider a photon beam with occupation number of the form

$$N = N(k) b(\bar{\theta}), \quad b(\bar{\theta}) = \exp\left(-\frac{\bar{\theta}^2}{2\bar{\theta}_0^2}\right), \quad (3.14)$$

where we assume $\bar{\theta}_0 \ll 1$. Since $b(\bar{\theta})$ makes a negligible contribution to the integrations in (3.13a, b) for large $\bar{\theta}$, the photon beam can be regarded as being effectively confined to an angle $\bar{\theta}_0 \ll 1$. The angular integrations in (3.13a, b) can be carried out if \bar{u} is approximately independent of the angles $(\bar{\theta}, \bar{\phi})$. One obtains

$$\Gamma_k = - \left(\frac{\pi}{2}\right)^{1/2} \int \frac{k dk}{(2\pi)^2} \frac{\bar{u} N(k)}{c} \frac{d \ln N(k)}{d \ln k} \bar{\theta}_0 \cot \chi_0 b(\bar{\theta}_2 - \chi_0), \quad (3.15a)$$

$$\Gamma_a = \left(\frac{\pi}{2}\right)^{1/2} \int \frac{k dk}{(2\pi)^2} \frac{\bar{u} N(k)}{c} \frac{\bar{\theta}_2 - \chi_0}{\bar{\theta}_0} b(\bar{\theta}_2 - \chi_0). \quad (3.15b)$$

From (3.15a, b), the conditions for $\Gamma_k < 0$ and $\Gamma_a < 0$ are $d \ln N / d \ln k > 0$ and $\bar{\theta}_2 < \chi_0$ respectively. The growth due to the anisotropic angular distribution of the beam dominates if $|\Gamma_a| \gg |\Gamma_k|$, that is,

$$\bar{\theta}_0 \left| \frac{d \ln N}{d \ln k} \right| \cot \chi_0 \ll \left| \frac{\bar{\theta}_2 - \chi_0}{\bar{\theta}_0} \right|. \quad (3.16)$$

The maximum growth Γ_a occurs at $\bar{\theta}_2 - \chi_0 \approx -\bar{\theta}_0$. Substituting $\bar{\theta}_2 - \chi_0 = -\bar{\theta}_0$ into (3.15a, b) and using $b(\bar{\theta}_2 - \chi_0) = e^{-1/2}$, we obtain

$$\Gamma_k = - \left(\frac{\pi}{2e}\right)^{1/2} \int \frac{k dk}{(2\pi)^2} \frac{\bar{u} N}{c} \frac{d \ln N}{d \ln k} \bar{\theta}_0 \cot \chi_0, \quad (3.17a)$$

$$\Gamma_a = - \left(\frac{\pi}{2e} \right)^{1/2} \int \frac{k dk}{(2\pi)^2} \frac{\bar{u}N}{c}. \quad (3.17b)$$

The condition (3.16) then becomes

$$\bar{\theta}_0 \left| \frac{d \ln N}{d \ln k} \right| \cot \chi_0 \ll 1. \quad (3.18)$$

In the following discussion we consider only the case where the conditions (3.18) and $\bar{\theta} < \chi_0$ are satisfied; that is, we consider only low-frequency wave growth due to the anisotropic angular distribution of the photon beam.

4. Growth rate for the x mode

In discussing the possible growth of low-frequency waves due to a photon beam passing through a cold, magnetized, electron–positron plasma, we need to consider three possibilities for the low-frequency waves: they may be in the x mode or the o mode or longitudinal. We discuss growth of the x mode first.

The ratio of the electric energy to the total energy in the low-frequency x -mode waves, R_{2x} , is given by (2.10) with all quantities corresponding to that for the low-frequency waves. For a weak magnetic field $\omega \gg \Omega_e$, retaining only the first term in (2.16) and using $\mathbf{e}_2 = \hat{\mathbf{a}}_2$, one finds

$$\begin{aligned} R_{2x} |e_i^* e_{1j} e_{2l} \alpha_{ijl}|^2 &\approx \frac{\varepsilon_0^2 e^2 \omega_p^4}{8m_e^2 c^2} \frac{n_{2x}^2 \Omega_e^2 \omega_2^2}{(\omega_2^2 - \Omega_e^2)^2 + \omega_p^2 \Omega_e^2} \sin^2 \theta_2 \\ &= \frac{\varepsilon_0^2 e^2 \omega_p^2 \omega_2^2}{8m_e^2 c^2} \frac{n_{2x}^2 (1 - n_{2x}^2)^2 \Omega_e^2}{\omega_p^2 + (1 + n_{2x}^2)^2 \Omega_e^2} \sin^2 \theta_2, \end{aligned} \quad (4.1)$$

which is valid for any ϕ_2 . The final expression in (4.1) is derived by using the refractive index (2.9) (denoted by $n_{2x} = k_2 c / \omega_2$) for the low-frequency x -mode waves. We assume that the scattered and unscattered waves have $|\mathbf{e}^* \cdot \mathbf{e}_1| \approx 1$. Using (4.1) and (3.12), one obtains the probability

$$\begin{aligned} \bar{u}_x &= \frac{4\hbar R R_1 R_{2x} |\alpha|^2}{\varepsilon_0^3 \omega^2 \omega_2} \\ &= r_e c^2 \frac{\pi \hbar \omega_2}{2m_e c^2} \left(\frac{\omega_p}{\omega} \right)^2 \frac{n_{2x}^2 (1 - n_{2x}^2)^2 \Omega_e^2}{\omega_p^2 + (1 - n_{2x}^2)^2 \Omega_e^2} \sin^2 \theta_2, \end{aligned} \quad (4.2)$$

where $r_e = e^2 / 4\pi \varepsilon_0 m_e c^2$ is the classical radius of the electron and $\alpha \equiv e_i^* e_{1j} e_{2l} \alpha_{ijl}$. In deriving (4.2), we assume $R \approx R_1 = \frac{1}{2}$.

The probability (4.2) is non-zero only for $n_{2x} > 1$ because the three-wave beat condition cannot be satisfied for $n_{2x} < 1$. The reason for this is the same as that for Čerenkov emission by a particle being possible only for refractive index greater than unity: the phase speed of the emitted wave must be less than the speed of the particle, which is replaced by the group speed of the photons in the present case. It follows that growth occurs only for the low-frequency x mode with frequency below the stop band, i.e. $\omega_2 < \Omega_e$. Because of the factor $(1 - n_{2x}^2)^2$ in the numerator in (4.2), fast growth requires that n_{2x}^2 differ significantly from unity.

The dependence on angle, $\bar{u} \propto \sin^2 \theta_2$, implies that any growth favours low-frequency waves propagating perpendicularly to the magnetic field. One may express (4.2) in terms of $\bar{\theta}_2$ and $\bar{\phi}_2$ as in (3.13a, b), using the spherical-triangular

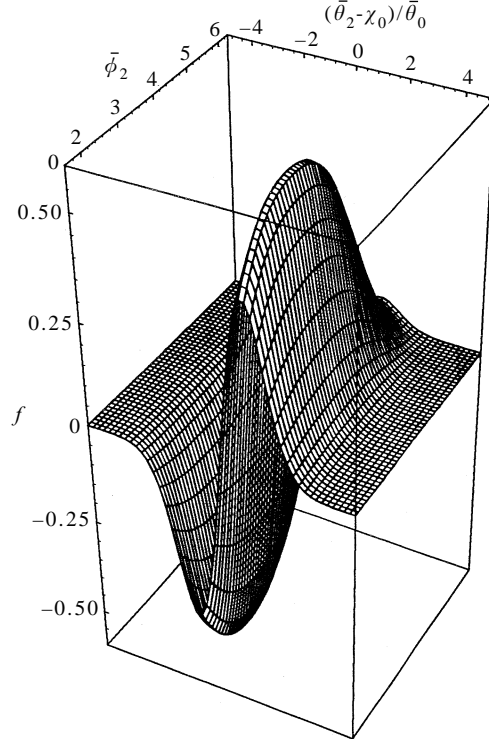


Figure 3. Plot of f as a function of $(\bar{\theta}_2 - \chi_0)/\bar{\theta}_0$ and $\bar{\phi}_2$ for low-frequency x -mode waves in a weak magnetic field. We choose $\theta_0 = \frac{1}{6}\pi$, $\bar{\theta}_0 = 10^{-2}$, $\omega_p^2/\omega_2^2 = 4$ and $\Omega_e/\omega_2 = 2$.

relation

$$\sin^2 \theta_2 = \sin^2 \bar{\theta}_2 \sin^2 \bar{\phi}_2 + (\cos \bar{\theta}_2 \sin \theta_0 - \sin \bar{\theta}_2 \cos \theta_0 \cos \bar{\phi}_2)^2, \quad (4.3)$$

where we assume that the axis of the photon beam is in the (x, z) plane and at an angle θ_0 to the field line. To evaluate the absorption coefficient (3.15 b), we assume a power-law distribution $N(k) \propto k^{-(\alpha+3)}$. Let $\Phi(\bar{\theta}_2, \bar{\phi}_2)$ represent the right-hand side of (4.3). When the angular spread of the photon beam is sufficiently small, i.e. the condition (3.18) is satisfied, the absorption coefficient is then $\Gamma \approx \Gamma_a$; that is,

$$\Gamma(\omega_2, \bar{\theta}_2, \bar{\phi}_2) = \left(\frac{\pi}{2}\right)^{1/2} \frac{r_e \omega_p^2}{c} \frac{T_B}{m_e c^2} \frac{\omega_2}{\omega} \frac{n_{2x}^2 (1 - n_{2x}^2)^2 \Omega_e^2}{\omega_p^2 + (1 - n_{2x}^2)^2 \Omega_e^2} \frac{n^2 f(\bar{\theta}_2, \bar{\phi}_2)}{8\pi(\alpha + 1)}, \quad (4.4a)$$

$$f(\bar{\theta}_2, \bar{\phi}_2) = \frac{\bar{\theta}_2 - \chi_0}{\bar{\theta}_0} \Phi(\bar{\theta}_2, \bar{\phi}_2) \exp\left[-\frac{(\bar{\theta}_2 - \chi_0)^2}{2\bar{\theta}_0^2}\right], \quad (4.4b)$$

where $\chi_0 = \arccos(1/n_{2x})$ and we assume $n_{2x} > 1$. The brightness temperature of the photons is defined by $T_B = \hbar\omega N(k)$.

Plots of $f(\bar{\theta}_2, \bar{\phi}_2)$ are given in Fig. 3. The growth region is for $f < 0$. This region is confined to a small meridional angle $\Delta\bar{\theta}_2 \approx 2\bar{\theta}_0$ and a relatively large azimuthal angle $\Delta\bar{\phi}_2 \gg \bar{\theta}_0$. For small θ_0 , one has $\Phi(\bar{\theta}_2, \bar{\phi}_2) \approx \sin^2 \theta_2$, and $f(\bar{\theta}_2, \bar{\phi}_2)$ is approximately independent of $\bar{\phi}_2$.

For a strong magnetic field $\omega \ll \Omega_e$, from (2.17) we have

$$|\alpha|^2 = \frac{\varepsilon_0^2 e^2 \omega_p^4}{m_e^2 c^2} \left(\frac{n_{2x} \omega_2}{\Omega_e} \right)^2 e_z^2 \sin^2 \theta, \quad (4.5)$$

with $e_z = \mathbf{e} \cdot \hat{\mathbf{B}}$. For $Y = \Omega_e/\omega_2 \gg 1$, we have $R_{2x} = \frac{1}{2}$, and it follows that $R_2^x |\alpha|^2$ is smaller than (4.1) by a factor $(\omega_2/\Omega_e)^2 \ll 1$. Thus the corresponding growth rate is much smaller than (4.4a).

When the frequency ω of high-frequency photons is close to the cyclotron frequency, $|\omega^2 - \Omega_e^2| \ll 2\omega\omega_2$, from (2.19) we obtain

$$|\alpha|^2 = \frac{\varepsilon_0^2 e^2 \omega_p^4}{4m_e^2 c^2} \left(\frac{n\omega\Omega_e}{\omega^2 - \Omega_e^2} \right)^2 |P|^2, \quad (4.6)$$

with

$$P = \left[-\frac{n_{2x}}{n} \hat{k}_{2r} (d_{ir} \varepsilon_{sjl} + d_{sj} \varepsilon_{irl}) \hat{B}_l + d_{ij} \hat{a}_s \sin \theta \right] e_i e_j \hat{a}_{2s}. \quad (4.7)$$

The first term in (2.19) does not contribute: this is because the projection of the polarization vector for the low-frequency x mode along $\hat{\mathbf{B}}$ gives zero. In the cyclotron-resonance regime, from (2.10) the ratio of the electric to total energy in high-frequency waves is

$$R \approx \frac{(\omega^2 - \Omega_e^2)^2}{\omega_p^2 \Omega_e^2}. \quad (4.8)$$

Multiplying (4.6) by (4.8), we obtain

$$R|\alpha|^2 = \frac{\varepsilon_0^2 e^2 \omega_p^2 \omega^2}{8m_e^2 c^2} n_{2x}^2 |P|^2. \quad (4.9)$$

To calculate the probability (3.12), we further assume $R_2 \approx \frac{1}{2}$ (which can be satisfied if $\omega_p^2/\omega_2^2 < 1$ and $Y = \Omega_e^2/\omega_2^2 \gg 1$) and $R_1 \approx \frac{1}{2}$. The angular dependence $|P|^2$ can be evaluated by considering a photon beam with polarization along $\hat{\mathbf{a}}$. Then we obtain

$$|P|^2 = \left[\sin \theta \cos(\phi_2 - \phi) + \frac{n_{2x}}{n} \sin \theta_2 \right]^2. \quad (4.10)$$

When high- and low-frequency waves all propagate along \mathbf{B} , one has $P = 0$ and hence $R|\alpha|^2 = 0$. To calculate the absorption coefficient, the angular dependence should be expressed in terms of $\bar{\theta}_2$ and $\bar{\phi}_2$ using the relations (4.3) and

$$\cos(\phi_2 - \phi) \approx \frac{\cos \chi_0 - \cos \theta_0 \cos \theta_2}{\sin \theta_0 \sin \theta_2}, \quad (4.11)$$

where $\cos \theta_2 = \cos \theta_0 \cos \bar{\theta}_2 - \sin \theta_0 \sin \bar{\theta}_2 \cos \bar{\phi}_2$. The absorption coefficient is then written in a form similar to (4.4a):

$$\Gamma(\omega_2, \bar{\theta}_2, \bar{\phi}_2) = \left(\frac{\pi}{2} \right)^{1/2} \frac{r_e \omega_p^2}{c} \frac{T_B}{m_e c^2} \frac{\omega}{\omega_2} \frac{n^4 f(\bar{\theta}_2, \bar{\phi}_2)}{8\pi(\alpha + 1)}, \quad (4.12)$$

with $f(\bar{\theta}_2, \bar{\phi}_2)$ given by (4.4b) and $\Phi(\theta_2, \phi_2) = |P|^2$ (which is then re-expressed in terms of $\bar{\theta}_2$ and $\bar{\phi}_2$).

Since $\Omega_e/\omega_2 \gg 1$, the condition $n_{2x} > 1$ can be satisfied automatically (cf. (2.9)). From (3.18), we have $\bar{\theta}_0 \ll (n_{2x}^2 - 1)^{1/2}/(\alpha + 1) = (\omega_p/\Omega_e)/(\alpha + 3)$. Thus, compared with the weak magnetic case, the growth rate is greater than (4.4a) (by about a

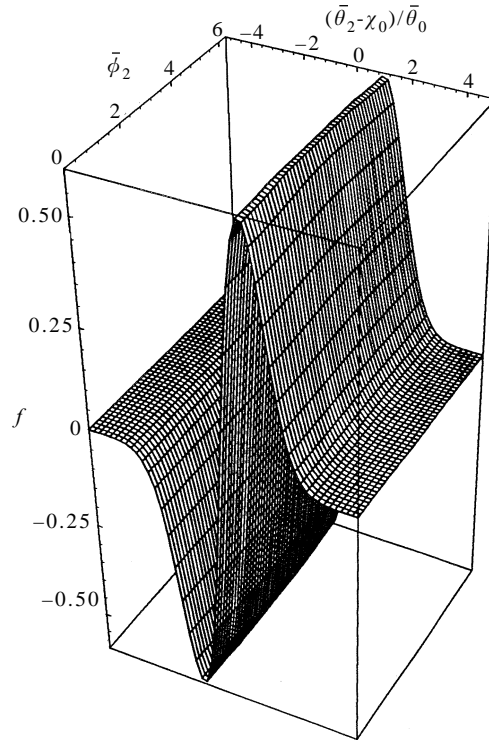


Figure 4. As Fig. 3, but with $\omega \approx \Omega_e$. We choose $\chi_0 = 10^{-2}$, $\bar{\theta}_0 = 10^{-5}$ and $n_{2x}/n \approx 1$.

factor $\omega^2/\omega_2^2 \gg 1$), but the growth can occur only when the angular spread of the photon beam is sufficiently small, $\bar{\theta}_0 \ll (\omega_p/\Omega_e)/(\alpha + 3)$. Since n_{2x} is close to unity (since $\Omega_e/\omega_2 \gg 1$) and $\chi_0 \ll 1$, it follows from (4.3), (4.10) and (4.11) that the growth is not axisymmetric with respect to \mathbf{B} , but is approximately axisymmetric with respect to $\hat{\mathbf{k}}_0$ (the photon beam axis). Figure 4 shows a plot of $f(\bar{\theta}_2, \bar{\phi}_2)$ with $\chi_0 = 10^{-2}$.

5. Growth rate for the *o* mode

For the *o* mode, in the weak-field approximation, since the polarization vector of the low-frequency *o* mode is in the $(\hat{\tau}_2, \hat{\mathbf{k}}_2)$ plane, we have $\mathbf{e}_2 \cdot \hat{\mathbf{a}}_2 = 0$, and hence the right-hand side of (2.16) does not contribute to the probability. To calculate α , terms of order ω_2^2/ω^2 in (A 3) and (A 4) need to be included, which implies that $|\alpha|^2 \propto \omega_2^4/\omega^4$. As $\omega_2/\omega \ll 1$, the growth of the low-frequency *o* mode in a weak magnetic field is much slower than the *x*-mode counterpart.

For a strong field (in the non-cyclotron-resonant case), $|\alpha|^2$ can be evaluated in a way similar to that for (4.5) by using (2.17). For linear polarization \mathbf{e} , the first and second terms in (2.17) are of order ω_2/ω . Hence, except for a factor of angular dependence, $|\alpha|^2$ is the same as (4.5), i.e. it is proportional to ω_2^2/Ω_e^2 . Thus the corresponding growth is ineffective.

For a photon beam with frequency near cyclotron resonance, $|\omega^2 - \Omega_e^2| \ll 2\omega\omega_2$,

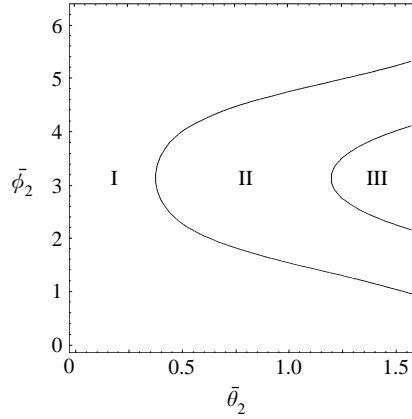


Figure 5. Solid-angular ranges for $n_{2o}^2 > 0$ (I, III) and $n_{2o}^2 < 0$ (II), with $\omega_p^2/\omega_2^2 = 2.5$.

and polarization along $\hat{\mathbf{a}}$, we can write $|\alpha|^2$ in the form (4.6), namely

$$|\alpha|^2 = \frac{\varepsilon_0^2 e^2 \omega_p^4}{4m_e^2 c^2} \left(\frac{n\omega\Omega_e}{\omega^2 - \Omega_e^2} \right)^2 \frac{\sin^2(\phi_2 - \phi)}{(1 - X)^2 \cos^2 \theta_2 + \sin^2 \theta_2} \times \left[\frac{n_{2o}}{n} \cot \theta \sin^2 \theta_2 - (1 - X) \cos \theta_2 \sin \theta \right]^2, \quad (5.1)$$

with $n_{2o} = k_2 c/\omega_2$. The first term in the square brackets is from the first term in (2.19), which can be derived as follows. For a linear polarization \mathbf{e} , we have

$$e_i e_{1j} \varepsilon_{ijl} \hat{B}_l = -e_i k_{2s} \left[\frac{\partial \mathbf{e}}{\partial k_s} \times \hat{\mathbf{B}} \right]_i, \quad (5.2)$$

where $\mathbf{e}_1 \approx \mathbf{e} - k_{2s} \partial \mathbf{e} / \partial k_s$. As we assume that $\mathbf{e} = \hat{\mathbf{a}}$ (which depends only on ϕ), we have $k_{2s} (\partial \mathbf{e} / \partial k_s) \times \hat{\mathbf{B}} = [\mathbf{k}_2 \cdot \hat{\mathbf{a}} / (k \sin \theta)] \hat{\mathbf{a}} = (\omega_2/\omega)(n_{2o}/n)(\mathbf{k}_2 \cdot \hat{\mathbf{a}}/\sin \theta) \hat{\mathbf{a}}$. The probability (3.12) can be calculated from (5.1), using the ratio (4.8) for the high-frequency waves and (2.13) for the low-frequency o -mode waves. The growth rate has a similar form to (4.12), but with

$$\Phi(\theta_2, \phi_2) = \frac{\sin^2(\phi_2 - \phi)}{(1 - X)^2 \cos^2 \theta_2 + \sin^2 \theta_2} \times \left[\frac{n_{2o}}{n} \cot \theta \sin^2 \theta_2 - (1 - X) \cos \theta_2 \sin \theta \right]^2. \quad (5.3)$$

Since (5.3) depends on ϕ_2 , the growth is not axisymmetric with respect to both \mathbf{B} and $\hat{\mathbf{k}}_0$. The angular function (5.3) can be written in terms of $\bar{\theta}_2$ and $\bar{\phi}_2$ using (4.3) and (4.11). For $\Omega_e/\omega_2 \gg 1$, the refractive index for the low-frequency o mode is approximated by $n_{2o}^2 = (X - 1)/(X \cos \theta_2 - 1)$, and wave propagation is allowed only in certain angular ranges (as shown in Fig. 5). Since the absorption coefficient is proportional to $\sin^2(\phi_2 - \phi)$, there are two growth peaks in general. Figure 6 shows one of the two peaks (growth corresponds to $f < 0$).

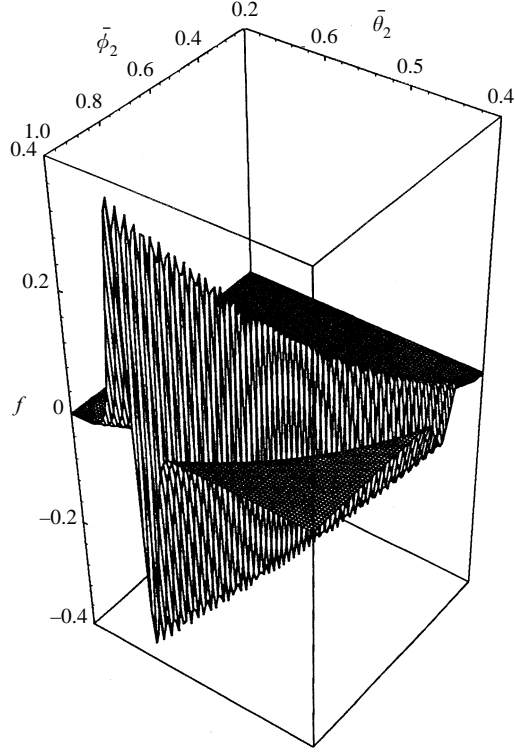


Figure 6. Plot of f as a function of $\bar{\theta}_2$ and $\bar{\phi}_2$. We choose $\bar{\theta}_0 = 10^{-2}$, $\theta_0 = \frac{1}{4}\pi$, $n \approx 1$ and $\omega_p^2/\omega_2^2 = 2.5$.

6. Growth rate for the longitudinal mode

For the longitudinal mode, we first consider the case $\omega \gg \Omega_e$. Since one has $\mathbf{e}_2 = \hat{\mathbf{k}}_2$, (2.16) is zero, and thus $|\alpha|^2$ is of order ω_2^4/ω^4 . As for low-frequency o -mode waves, the growth of longitudinal waves in the weak magnetic field is not effective. This is in contrast with ordinary electron-ion plasmas, in which growth of longitudinal waves is favoured (see e.g. Melrose 1994).

For a strong magnetic field, similarly to (4.5), we have $|\alpha|^2 \propto \omega^2/\Omega_e^2$. As $\omega^2/\Omega_e^2 \ll 1$, the corresponding growth is much weaker than for ordinary electron-ion plasmas.

For a strong magnetic field and $\Omega_e \sim \omega \gg \omega_2$, scattering may occur in the resonance regime (Luo and Melrose 1994). The quantity $R|\alpha|^2$ was derived by Luo and Melrose (1994) for $\mathbf{k}_2 \parallel \mathbf{B}$ (cf. (6) in their paper). Here we consider the case in which high-frequency photon beam is linearly polarized with polarization vector $\mathbf{e} = \hat{\mathbf{a}}$, and thus the first (antisymmetric) term in (2.19) is proportional to ω_2/ω . This term appears in α as $(\omega_2/\omega)(n_{2l}/2n) \cot \theta \sin(2\theta_2) \sin(\phi_2 - \phi)$, where n_{2l} is the refractive index for the low-frequency longitudinal waves. Since $e_i d_{ir} \approx e_r$, among all terms in the square brackets in (2.19) only the last term contributes to α . Following the same procedure as for deriving (5.1), $|\alpha|^2$ is evaluated to be

$$|\alpha|^2 = \frac{\varepsilon_0^2 e^2 \omega_p^4}{4m_e^2 c^2} \left(\frac{n\omega\Omega_e}{\omega^2 - \Omega_e^2} \right)^2 \left(\frac{n_{2l}}{n} \cot \theta \cos \theta_2 + \sin \theta \right)^2 \sin^2 \theta_2 \sin^2(\phi_2 - \phi). \quad (6.1)$$

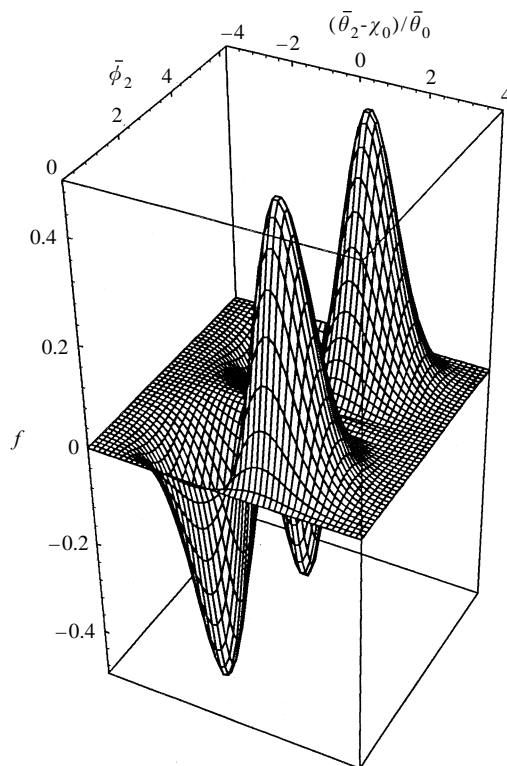


Figure 7. Plot of f as a function of $(\bar{\theta}_2 - \chi_0)/\bar{\theta}_0$ and $\bar{\phi}_2$ for low-frequency longitudinal waves when the frequency of the high-frequency photons is close to the cyclotron frequency. We choose $\chi_0 = \frac{1}{4}\pi$, $\bar{\theta}_0 = 10^{-2}$, $\theta_0 = \frac{1}{4}\pi$ and $n_{2l}/n \approx 1$.

The absorption coefficient can be derived from (6.1) together with the ratio (4.8) and expressed into the same form as (4.12) but with

$$\Phi = [(n_{2l}/n) \cot \theta \cos \theta_2 + \sin \theta]^2 \sin^2 \theta_2 \sin^2(\phi_2 - \phi). \quad (6.2)$$

When $\omega_p^2/\omega_2^2 < 1$ and $Y = \Omega_e/\omega_2 \gg 1$, we may assume that $R_1 \approx \frac{1}{2}$ and $R_{2l} \approx \frac{1}{2}$ (cf. (2.15) for the low-frequency longitudinal waves). Since (6.1), (4.6) and (5.3) are all similar to each other (except for the angular dependence), the corresponding absorption coefficient calculated from (6.1) is comparable with those for the x and o modes under similar conditions (e.g. $\omega \approx \Omega_e$). Figure 7 shows the angular function $f(\bar{\theta}_2, \bar{\phi}_2)$. Growth occurs in the solid-angular range where $f < 0$. The figure shows two growth peaks.

7. Conclusions

We have investigated photon-beam-induced instabilities of various low-frequency waves in a charge-neutral electron–positron plasma in the random-phase approximation. In summarizing the properties of waves in a cold, magnetized, electron–positron plasma, we note (a) that such a plasma is non-gyrotropic, (b) that the wave properties can be derived by analogy with those for a uniaxial crystal, and (c) that in the special cases of parallel and perpendicular propagation different wave properties are obtained depending on whether one takes the limits as $\theta \rightarrow 0$ and

$\theta \rightarrow \frac{1}{2}\pi$ before taking the limit as $\xi \rightarrow 0$ (ξ is a measure of the charge imbalance) or vice versa.

We have discussed the small-angle scattering regime in which the occupation number of relevant low-frequency waves is much smaller than that of high-frequency waves. With this approximation, wave–wave interactions are treated by analogy with wave–particle interactions. Specifically, we have considered photon-beam-induced low-frequency wave instabilities, and have calculated the corresponding absorption coefficients in the cold-plasma approximation. Our main conclusions are as follows.

- (i) Three-wave interactions in electron–positron plasmas depend strongly on the magnetic field. For an unmagnetized electron–positron plasma in which electrons and positrons have the same distribution, three-wave interactions are forbidden (one has $\alpha_{ijl} = 0$ and $\bar{u}(\mathbf{k}, \mathbf{k}_1, \mathbf{k}_2) = 0$). We have concentrated here on effects associated with the non-zero contribution that arises from the presence of an ambient magnetic field. Thus, throughout our discussion, we have assumed a neutral pair plasma ($\xi = 0$) and that, apart from an arbitrary phase, the polarization vectors of high-frequency waves are real.
- (ii) Instabilities of low-frequency waves due to a high-frequency photon beam occur only in a certain solid-angular range of \mathbf{k}_2 , which has a wide span in azimuthal angle $\Delta\phi_2 \gg \bar{\theta}_0$ and a much narrower one in meridional angle $\Delta\bar{\theta}_2 \approx 2\bar{\theta}_0$. For a strong magnetic field, the growth is not axisymmetric with respect to either \mathbf{B} or the photon beam axis in general. For *o*- and longitudinal-mode waves, there are two growth peaks at two different azimuthal angles (as shown in Fig. 7, while Fig. 6 only shows one of the two). For a weak magnetic field, growth is approximately axisymmetric about \mathbf{B} (i.e. there is no ϕ_2 dependence in (4.1) and (4.2)).
- (iii) For both low-frequency longitudinal- and *o*-mode waves, growth is not effective in a weak magnetic field ($\omega \gg \Omega_e, \omega_2$), but growth of all three modes (longitudinal, *o* and *x* mode) is significantly enhanced in the cyclotron-resonance regime, where the photon frequency is close to the cyclotron frequency. For low-frequency *x*-mode waves, since the refractive index n_{2x} given by (2.9) is very close to unity for $\omega_2 \ll \Omega_e \approx \omega$ and $\Omega_e \gg \omega_p$, growth can occur only when the angular spread of the photon beam is sufficiently narrow, i.e. for $\bar{\theta}_0 \ll (\omega_p/\Omega_e)/(\alpha + 3)$.
- (iv) For *x*-mode waves, three-wave interactions can be important in a weak magnetic field ($\omega \gg \Omega_e \approx \omega_2$). Since the condition for any growth is $\omega_2 - \mathbf{k}_2 \cdot \mathbf{v}_g = 0$, growth for low-frequency waves occurs only for $n_2 > 1$. For low-frequency *x*-mode waves, this requires that the frequency ω_2 be below the stop band, implying that growth does not occur for $\omega_2 > \Omega_e$. Because the growth rate is proportional to $(1 - n_{2x}^2)^2$, for fast growth to occur the refractive index n_{2x} must differ significantly from unity. For both weak and strong magnetic fields, growth favours the perpendicular (to \mathbf{B}) direction.

Finally, we should remark that the result (iii) depends strongly on the cold-plasma approximation for the quadratic response tensor being valid. In practice, thermal effects tend to be important near a resonance, and tend to reduce the effect of a resonance. Our discussion is inconsistent in that we ignore the effect

of the cyclotron resonance on the wave properties for high-frequency photons, but retain it in the nonlinear response. A systematic investigation of this important case is required.

Acknowledgements

Q. Luo thanks Abraham C.-L. Chian for useful discussions, and FAPESP (Brazil) for financial support.

Appendix A

For $\xi = 0$, the quadratic response tensor (2.4) can be written into the form

$$\begin{aligned} \alpha_{ijs} = & -i \frac{\varepsilon_0 e \omega_p^2}{2m_e c} \left\{ \frac{kc}{\omega_1} \frac{\omega_1^2}{\omega_1^2 - \Omega_e^2} \frac{\omega_2^2}{\omega_2^2 - \Omega_e^2} \hat{k}_r \left[d_{rj}(\omega_1) \frac{\Omega_e}{\omega_2} \varepsilon_{isl} + \frac{\Omega_e}{\omega_1} \varepsilon_{rjl} d_{is}(\omega_2) \right] \right. \\ & + \frac{kc}{\omega_2} \frac{\omega_1^2}{\omega_1^2 - \Omega_e^2} \frac{\omega_2^2}{\omega_2^2 - \Omega_e^2} \hat{k}_r \left[d_{rs}(\omega_2) \frac{\Omega_e}{\omega_1} \varepsilon_{ijl} + \frac{\Omega_e}{\omega_2} \varepsilon_{rsl} d_{ij}(\omega_1) \right] \\ & + \frac{k_1 c}{\omega} \frac{\omega^2}{\omega^2 - \Omega_e^2} \frac{\omega_2^2}{\omega_2^2 - \Omega_e^2} \hat{k}_{1r} \left[d_{ir}(\omega) \frac{\Omega_e}{\omega_2} \varepsilon_{jsl} + \frac{\Omega_e}{\omega} \varepsilon_{irl} d_{js}(\omega_2) \right] \\ & + \frac{k_2 c}{\omega} \frac{\omega^2}{\omega^2 - \Omega_e^2} \frac{\omega_1^2}{\omega_1^2 - \Omega_e^2} \hat{k}_{2r} \left[d_{ir}(\omega) \frac{\Omega_e}{\omega_1} \varepsilon_{sjl} + \frac{\Omega_e}{\omega} \varepsilon_{irl} d_{sj}(\omega_1) \right] \\ & - \frac{k_2 c}{\omega_1} \frac{\omega^2}{\omega^2 - \Omega_e^2} \frac{\omega_1^2}{\omega_1^2 - \Omega_e^2} \hat{k}_{2r} \left[d_{rj}(\omega_1) \frac{\Omega_e}{\omega} \varepsilon_{isl} + \frac{\Omega_e}{\omega_1} \varepsilon_{rjl} d_{is}(\omega) \right] \\ & \left. - \frac{k_1 c}{\omega_2} \frac{\omega^2}{\omega^2 - \Omega_e^2} \frac{\omega_2^2}{\omega_2^2 - \Omega_e^2} \hat{k}_{1r} \left[d_{rs}(\omega_2) \frac{\Omega_e}{\omega} \varepsilon_{ijl} + \frac{\Omega_e}{\omega_2} \varepsilon_{rsl} d_{ij}(\omega) \right] \right\} \hat{B}_l, \quad (\text{A } 1) \end{aligned}$$

$$d_{ij}(\omega) = \delta_{ij} - \frac{\Omega_e^2}{\omega^2} \hat{B}_i \hat{B}_j, \quad (\text{A } 2)$$

The relevant approximation is $\omega \approx \omega_1 \gg \omega_2$. We consider three cases: $\omega \gg \Omega_e$, $\omega_2 \ll \Omega_e$ and $\omega \approx \Omega_e$.

For the weak-field approximation, we expand (A 1) in terms of $\omega_2/\omega \ll 1$, $\Omega_e/\omega \ll 1$. Thus the fourth and fifth terms in the curly brackets are proportional to $\omega_2 \Omega_e/\omega^2$, and are ignored. Also, the final term in (A 2) is ignored for the high-frequency waves. In calculating the probability, the quadratic response tensor appears in the form $\alpha = e_i^* e_{1j} \alpha_{ijs} e_{2s}$, and, with the high-frequency waves assumed transverse, one has $\mathbf{e} \cdot \mathbf{k} = 0 = \mathbf{e}_1 \cdot \mathbf{k}_1$. Then, using $\mathbf{k} = \mathbf{k}_1 + \mathbf{k}_2$, one has $\hat{\mathbf{k}} \cdot \mathbf{e}_1 \approx (k_2/k) \hat{\mathbf{k}}_2 \cdot \mathbf{e}$ and $\hat{\mathbf{k}}_1 \cdot \mathbf{e} \approx -(k_2/k) \hat{\mathbf{k}}_2 \cdot \mathbf{e}$. Using these approximations, the first and third terms together give

$$\frac{n_2 \omega_2 \Omega_e}{\omega_2^2 - \Omega_e^2} \frac{\omega_2}{\omega} \left[\frac{n}{n_2} \hat{k}_r (\varepsilon_{irl} d_{js} + \varepsilon_{rjl} d_{is}) + (\hat{k}_{2j} \varepsilon_{isl} \hat{B}_l - \hat{k}_{2i} \varepsilon_{jsl} \hat{B}_l) \right], \quad (\text{A } 3)$$

with $d_{ij} = d_{ij}(\omega_2)$. The second and sixth terms together give

$$\frac{n_2 \omega_2 \Omega_e}{\omega_2^2 - \Omega_e^2} \left[\hat{k}_{2r} \varepsilon_{rsl} \hat{B}_l \delta_{ij} + \frac{\omega_2}{\omega} \left(\frac{n}{n_2} \hat{k}_r + \hat{k}_{2r} \right) d_{rs} \varepsilon_{ijl} \hat{B}_l \right]. \quad (\text{A } 4)$$

Note that in (A 3) and (A 4) the difference between i and j in contracting with

the polarization vectors is of order $k_2/k \ll 1$, and thus $\varepsilon_{irl}d_{js} + \varepsilon_{rjl}d_{is} = O(k_2/k)$. Compared with the first term in (A 4), all terms in (A 3) and the second term in (A 4) are of order ω_2^2/ω^2 . Using $\hat{a}_{2s} \sin \theta_2 = \varepsilon_{slr}\hat{B}_l\hat{k}_{2r}$ and ignoring terms of order ω_2^2/ω^2 , the first term in (A 4) (multiplied by $-i\varepsilon_0 e\omega_p^2/2m_e c$) leads to (2.16).

For the strong-field case, we consider the conditions $\Omega_e \gg \omega_2$ and $|\omega^2 - \Omega_e^2| \gg 2\omega\omega_2 \gg \omega_2^2$. Then, using the expansions

$$d_{ij}(\omega_1) - d_{ij}(\omega) = -\frac{2\omega_2}{\omega} \frac{\Omega_e^2}{\omega^2} \hat{B}_i \hat{B}_j + \dots,$$

$$\frac{\omega_1^2}{\omega_1^2 - \Omega_e^2} = \frac{\omega^2}{\omega^2 - \Omega_e^2} \left(1 - \frac{2\omega_2}{\omega} + \frac{2\omega\omega_2}{\omega^2 - \Omega_e^2} + \dots \right),$$

we obtain

$$\alpha_{ijs} = -i \frac{\varepsilon_0 e \omega_p^2}{2m_e c} \left[\hat{k}_r (\varepsilon_{rjl} \hat{B}_i + \varepsilon_{irl} \hat{B}_j) \hat{B}_l \hat{B}_s \right. \\ \left. + \left(\frac{\omega^2 + \Omega_e^2}{\omega^2 - \Omega_e^2} \hat{k}_r + \frac{n_2}{n} \hat{k}_{2r} \right) \hat{B}_r \varepsilon_{ijl} \hat{B}_l \hat{B}_s + \frac{\omega_2}{\omega} P_{ijs} \right], \quad (\text{A } 5)$$

with

$$P_{ijs} = \frac{2\omega^2}{\omega^2 - \Omega_e^2} \left[\frac{n_2}{n} \hat{k}_{2r} (d_{ir} \varepsilon_{sjl} + d_{sj} \varepsilon_{irl}) \hat{B}_l - \delta_{\perp ij} \hat{k}_r \varepsilon_{rst} \hat{B}_l + \hat{k}_r \varepsilon_{rjl} \hat{B}_l \hat{B}_i \hat{B}_s \right] \\ - \frac{\omega^2}{\Omega_e^2} \left[2\hat{k}_r d_{rj} \varepsilon_{isl} + \frac{n_2}{n} d_{ij} \hat{k}_{2r} \varepsilon_{rst} \right] \hat{B}_l - \frac{n_2}{n} \hat{k}_{2r} \varepsilon_{irl} \hat{B}_l \hat{B}_j \hat{B}_s, \quad (\text{A } 6)$$

with $\delta_{\perp ij} \equiv \delta_{ij} - \hat{B}_i \hat{B}_j$. Using $\varepsilon_{irl} \hat{k}_r \hat{B}_l = -\hat{a}_i \sin \theta$, for $\omega/\Omega_e \ll 1$ we obtain (2.17).

Near the cyclotron resonance $\omega \approx \Omega_e$, $\omega_2^2 \ll |\omega^2 - \Omega_e^2| \ll 2\omega\omega_2$, the terms of $1/(\omega^2 - \Omega_e^2)$ dominate, and we have $\omega_1^2/(\omega_1^2 - \Omega_e^2) \approx -\omega/2\omega_2$. Then

$$\alpha_{ijs} = -i \frac{\varepsilon_0 e \omega_p^2}{2m_e c} \frac{n\omega\Omega_e}{\omega^2 - \Omega_e^2} \frac{\omega}{\omega_2} \left(-\hat{k}_r \hat{B}_r \varepsilon_{ijl} \hat{B}_l \hat{B}_s + \frac{\omega_2}{\omega} P_{ijs} \right), \quad (\text{A } 7)$$

$$P_{ijs} = \hat{k}_r \varepsilon_{irl} \hat{B}_l \hat{B}_j \hat{B}_s - \frac{n_2}{n} \hat{k}_{2r} (d_{ir} \varepsilon_{sjl} + d_{sj} \varepsilon_{irl}) \hat{B}_l \\ + \frac{n_2}{n} \hat{k}_{2r} \hat{B}_r \varepsilon_{ijl} \hat{B}_l \hat{B}_s + \varepsilon_{rst} \hat{B}_l d_{ij} \hat{k}_r. \quad (\text{A } 8)$$

Equation (2.19) follows from (A 7).

Appendix B

In kinetic theory, three-wave interactions can be described by a set of three kinetic equations (see e.g. Tsytovich 1977; Melrose 1986). When two of the three waves are in the same mode, the two equations for high-frequency waves can be combined into one equation:

$$\frac{dN(\mathbf{k})}{dt} = \int \frac{d^3 k_1}{(2\pi)^3} \frac{d^3 k_2}{(2\pi)^3} (u(\mathbf{k}, \mathbf{k}_1, \mathbf{k}_2) \{N(\mathbf{k}_1)N_L(\mathbf{k}_2) - N(\mathbf{k})[N(\mathbf{k}_1) + N_L(\mathbf{k}_2)]\} \\ - u(\mathbf{k}_1, \mathbf{k}, \mathbf{k}_2) \{N(\mathbf{k})N_L(\mathbf{k}_2) - N(\mathbf{k}_1)[N(\mathbf{k}) + N_L(\mathbf{k}_2)]\}), \quad (\text{B } 1)$$

where

$$u(\mathbf{k}, \mathbf{k}_1, \mathbf{k}_2) = \frac{4\hbar R R_1 R_2 |e_i^* e_{1j} e_{2l} \alpha_{ijl}|^2}{\varepsilon_0^3 \omega \omega_1 \omega_2} \times (2\pi)^4 \delta^3(\mathbf{k} - \mathbf{k}_1 - \mathbf{k}_2) \delta[\omega(\mathbf{k}) - \omega_1(\mathbf{k}_1) - \omega_2(\mathbf{k}_2)] \quad (\text{B } 2)$$

is the three-wave probability. The delta-functions are the three-wave beat conditions, which correspond to energy and momentum conservations in the semiclassical formalism. For the low-frequency wave mode, the kinetic equation is

$$\frac{dN_L(\mathbf{k}_2)}{dt} = - \int \frac{d^3 k}{(2\pi)^3} \frac{d^3 k_1}{(2\pi)^3} \times u(\mathbf{k}, \mathbf{k}_1, \mathbf{k}_2) \{N(\mathbf{k}_1)N_L(\mathbf{k}_2) - N(\mathbf{k})[N(\mathbf{k}_1) + N_L(\mathbf{k}_2)]\}, \quad (\text{B } 3)$$

On the right-hand sides of (B 1) and (B 3), the terms proportional to N_L correspond the process of induced emission of low-frequency waves, and the terms without N_L describe the process of induced photon decay. It is straightforward to carry out the integrations over $d^3 k_1$ in (B 1) and (B 3). This gives a condition $\mathbf{k}_1 = \mathbf{k} - \mathbf{k}_2$ for (B 3) and the first term in (B 1) and a condition $\mathbf{k}_1 = \mathbf{k} + \mathbf{k}_2$ for the second term in (B 1). The quasilinear equations (3.1) and (3.2) can be derived by expanding $u(\mathbf{k} + \mathbf{k}_2, \mathbf{k}, \mathbf{k}_2)$ and $N(\mathbf{k} \pm \mathbf{k}_2)$ as

$$u(\mathbf{k} + \mathbf{k}_2, \mathbf{k}, \mathbf{k}_2) \approx u(\mathbf{k}, \mathbf{k} - \mathbf{k}_2, \mathbf{k}_2) + \mathbf{k}_2 \cdot \frac{\partial}{\partial \mathbf{k}} u(\mathbf{k}, \mathbf{k}_1, \mathbf{k}_2) \Big|_{\mathbf{k}_1 = \mathbf{k} - \mathbf{k}_2} + \mathbf{k}_2 \cdot \frac{\partial}{\partial \mathbf{k}_1} u(\mathbf{k}, \mathbf{k}_1, \mathbf{k}_2) \Big|_{\mathbf{k}_1 = \mathbf{k} - \mathbf{k}_2}, \quad (\text{B } 4)$$

$$N(\mathbf{k} \pm \mathbf{k}_2) \approx N(\mathbf{k}) \pm \mathbf{k}_2 \cdot \frac{\partial}{\partial \mathbf{k}} N(\mathbf{k}) + \frac{1}{2} \left(\mathbf{k}_2 \cdot \frac{\partial}{\partial \mathbf{k}} \right)^2 N(\mathbf{k}). \quad (\text{B } 5)$$

To derive (3.1), it is sufficient to expand $N(\mathbf{k} \pm \mathbf{k}_2)$ up to first order in \mathbf{k}_2 .

Appendix C

To derive (3.13a, b), one may integrate over $\bar{\phi}$ in (3.11) to obtain

$$\int_0^{2\pi} d\bar{\phi} \delta(\cos \chi - \cos \chi_0) = \frac{1}{\sin \bar{\theta} \sin \bar{\theta}_2 \sin(\bar{\phi}_0 - \bar{\phi}_2)}, \quad (\text{C } 1)$$

where $\bar{\phi}_0$ satisfies the condition

$$\cos \bar{\theta} \cos \bar{\theta}_2 + \sin \bar{\theta} \sin \bar{\theta}_2 \cos(\bar{\phi}_0 - \bar{\phi}_2) = \cos \chi_0 = \frac{\omega_2}{k_2 v_g}.$$

We write

$$\sin \bar{\theta} \sin \bar{\theta}_2 \sin(\bar{\phi}_0 - \bar{\phi}_2) = [1 - \cos^2 \bar{\theta} - \cos^2 \bar{\theta}_2 - \cos^2 \chi_0 + 2 \cos \chi_0 \cos \bar{\theta}_2 \cos \bar{\theta}]^{1/2} \equiv F(\bar{\theta}, \bar{\theta}_2, \chi_0).$$

For a collimated photon beam, we assume $\bar{\theta} \ll 1$. We also assume $|\bar{\theta}_2 - \chi| \ll 1$. Then F can be expanded as

$$F(\bar{\theta}, \bar{\theta}_2, \chi_0) \approx [\bar{\theta}^2 - (\bar{\theta}_2 - \chi_0)^2]^{1/2} \sin \chi_0. \quad (\text{C } 2)$$

After integration over $\bar{\phi}$, (3.11) becomes

$$\Gamma = - \int d\bar{\theta} \sin \bar{\theta} \int \frac{k^2 dk}{(2\pi)^2} \frac{\bar{u}}{v_g [\bar{\theta}^2 - (\bar{\theta}_2 - \chi_0)^2]^{1/2} \sin \chi_0} \times \left(\cos \chi_0 \frac{\partial}{\partial k} + \frac{\cos \bar{\theta} \cos \chi_0 - \cos \bar{\theta}_2}{k \sin \bar{\theta}} \frac{\partial}{\partial \bar{\theta}} \right) N(k, \bar{\theta}). \quad (\text{C } 3)$$

The first term produces (3.13a) with $v_g \approx c$. The second term leads to (3.13b), using

$$\begin{aligned} \cos \bar{\theta}_2 - \cos \bar{\theta} \cos \chi_0 &= \cos \bar{\theta}_2 - \cos(\bar{\theta}_2 - \chi_0) \cos \chi_0 + O(\bar{\theta}^2) + O((\bar{\theta}_2 - \chi_0)^2) \\ &\approx -\sin(\bar{\theta}_2 - \chi_0) \sin \chi_0 \approx -(\bar{\theta}_2 - \chi_0) \sin \chi_0. \end{aligned}$$

References

- Gangadhara, R. T. and Krishan, V. 1993 *Astrophys. J.* **415**, 505.
 Gedalin, M. and Eichler, D. 1993 *Astrophys. J.* **406** 629.
 Gedalin, M. E. and Machabeli, G. Z. 1984 *Soviet J. Plasma Phys.* **9**, 592.
 Greaves, R. G., Tinkle, M. D. and Surko, C. M. 1994 *Phys. Plasmas* **1**, 1439.
 Istomin, Ya. N. 1988 *Soviet Phys. JETP* **67**, 1380.
 Iwamoto, M. 1993 *Phys. Rev.* **E47**, 604.
 Levinson, A. and Blandford, R. 1995 *Mon. Not. R. Astron. Soc.* **274**, 717.
 Luo, Q. and Melrose, D. B. 1994 *Solar Phys.* **154**, 187.
 Luo, Q. and Melrose, D. B. 1995a *Publ. Astron. Soc. Aust.* **12**, 71.
 Luo, Q. and Melrose, D. B. 1995b *Astrophys. J.* **452**, 346.
 Melrose, D. B. 1986 *Instabilities in Space and Laboratory Plasmas*. Cambridge University Press.
 Melrose, D. B. 1994 *J. Plasma Phys.* **51**, 13.
 Melrose, D. B. and McPhedran, R. C. 1991 *Electromagnetic Processes in Dispersive Media: A Treatment Based on the Dielectric Tensor*. Cambridge University Press.
 Mikhailovskii, A. B. 1980 *Soviet J. Plasma Phys.* **6**, 336.
 Stewart, G. A. and Laing, E. W. 1992 *J. Plasma Phys.* **47**, 295.
 Stix, T. H. 1962 *The Theory of Plasma Waves*. McGraw-Hill, New York.
 Stringer, T. E. 1963 *Plasma Phys.* **5**, 89.
 Surko, C. M., Leventhal, M. and Passner, A. 1989 *Phys. Rev. Lett.* **62**, 901.
 Tsytovich, V. N. 1977 *Theory of Turbulent Plasma*. Consultants Bureau, New York.
 Zank, G. P. and Greaves, R. G. 1995 *Phys. Rev.* **E51**, 6079.